Journal of Human Evolution 189 (2024) 103514

Contents lists available at ScienceDirect

Journal of Human Evolution

journal homepage: www.elsevier.com/locate/jhevol

Three-dimensional geometric morphometric analysis of the bony labyrinth of Xujiayao 6

Yameng Zhang [a,b], Alessandro Urciuoli [c,d,e,f,*], Clément Zanolli [g], Ottmar Kullmer [e,h], Xiujie Wu [i,*]

[a] Joint International Research Laboratory of Environmental and Social Archaeology, Shandong University, Qingdao, 266237, China
[b] Institute of Cultural Heritage, Shandong University, Qingdao, 266237, China
[c] Universitat Autònoma de Barcelona, Campus de la UAB, 08193 Cerdanyola del Vallès, Barcelona, Spain
[d] Institut Català de Paleontologia Miquel Crusafont (ICP-CERCA), Universitat Autònoma de Barcelona, Edifici ICTA-ICP, c/ Columnes s/n, 08193 Cerdanyola del Vallès, Barcelona, Spain
[e] Division of Palaeoanthropology, Senckenberg Research Institute and Natural History Museum Frankfurt, Senckenberganlage 25, 60325, Frankfurt am Main, Germany
[f] Universidad de Alcalá, Cátedra de Otoacústica Evolutiva y Paleoantropología (HM Hospitales-UAH), Departamento de Ciencias de la Vida, 28871, Alcalá de Henares, Madrid, Spain
[g] Univ. Bordeaux, CNRS, MCC, PACEA, UMR 5199, F-33600, Pessac, France
[h] Department of Paleobiology and Environment, Institute of Ecology, Evolution, and Diversity, Goethe University, Max-von-Laue-Str. 13, 60438 Frankfurt, Germany
[i] Key Laboratory of Vertebrate Evolution and Human Origins, Institute of Vertebrate Paleontology and Paleoanthropology, Chinese Academy of Sciences, Beijing, China

ARTICLE INFO

Handling editor: A Taylor

1. Introduction

In 1976, the first *Homo* fossils were found at the Xujiayao (XJY; also named Houjiayao) site locality 74093, Nihewan Basin, Northern China. Later excavations yielded a total of 21 cranial fragments, including 13 parietal bones, two occipital bones, one left temporal bone, one partial left maxilla, one partial mandible, and three isolated teeth (Wu et al., 2022). Recently, Wu et al. (2022) reconstructed the posterior portion of a cranium, XJY 6, with three of the fragments: a right parietal (originally PA 1490), an occipital (PA 1486), and a left temporal bone (PA 1498). A series of dating methods have been applied to the material from this site, resulting in various ages: 125–104 ka by uranium series (Chen et al., 1984), 200–160 ka by optically stimulated luminescence (Li et al., 2014), and 370–270 ka by electron spin resonance (Ao et al., 2017). The optically stimulated luminescence date is consistent with the cold-adapted fauna at the site and therefore more likely to be representative of the chronology of *Homo* in the site (Norton and Gao, 2008; Wu et al., 2022).

The examination of the XJY fossils reveals a mosaic morphological pattern, exhibiting a combination of both derived (Neanderthal- and modern human-like) and archaic features (as seen in some Early to Middle Pleistocene *Homo* specimens). Several anatomical traits of the XJY *Homo* were suggested to display a Neanderthals-like morphology (Wu et al., 2014). The XJY 1 maxilla displays a bilevel nasal floor (Franciscus, 2003; Wu et al., 2012), a broad and rounded nasal margin, and strongly shoveled maxillary central incisors and canines (Wu and Poirier, 1995; Liu et al., 2013; Wu and Trinkaus, 2014). The XJY 14 mandible features a wide mandibular ramus, an asymmetrical mandibular notch, an enlarged superior medial pterygoid tubercle, and a probable retromolar space (Wu and Trinkaus, 2014). The temporal bone of XJY 6 (originally designated as XJY 15) exhibits a high sagittal labyrinth index (i.e., the arc of the posterior canal is positioned low relative to the plane of the lateral canal; Spoor et al., 2003) and a relatively large lateral semicircular canal (Wu et al., 2014). However, the XJY remains also display characteristics that deviate from those typically observed in Neanderthals. The crowns of the M^1s show a subrectangular outline in occlusal view, a prominent cingular development, and peripherally situated cusps (Xing et al., 2015). The XJY 14 mandible possesses a mandibular gonial eversion and an open mandibular foramen (Wu and Trinkaus, 2014). The external morphology of the XJY 6 temporal bone bears little resemblance to that of Neanderthals, presenting a high and rounded squamosal portion. Additionally, the zygomatic arch extends

* Corresponding authors.
E-mail addresses: urciuoli.a@gmail.com (A. Urciuoli), wuxiujie@ivpp.ac.cn (X. Wu).

https://doi.org/10.1016/j.jhevol.2024.103514
Received 17 December 2023; Received in revised form 17 February 2024; Accepted 17 February 2024
Available online 27 March 2024

posteriorly above the auditory meatus, forming a supramastoid crest that terminates at the parietal notch. Notably, the long axis of the external acoustic meatus is oriented vertically rather than horizontally (Wu and Trinkaus, 2014).

Evidence from ancient DNA indicates that Neanderthals and Denisovans diverged approximately 550,000 to 765,000 years ago (Meyer et al., 2016), or between 800 ka and 1 Ma based on dental morphology (Gómez-Robles, 2019). Both ancient DNA and morphological data suggest that Sima de los Huesos hominins are likely among the earliest members of the Neanderthal lineage (Arsuaga et al., 2014; Meyer et al., 2014, 2016). However, in absence of genetic data and due to the apparent morphological variability observed in the eastern Asian Middle to Late Pleistocene fossil record, the phylogenetic relationships of most *Homo* fossils, such as XJY, Dali, Xuchang, and Jinniushan, with Denisovans and Neanderthals, remain unclear and this topic is currently under intense debate (Bae et al., 2023a, 2023b). Denisovans are the sister group of Neanderthals and, based on genetic analyses of living populations, it has been suggested that Denisovans lived in Asia, where they probably met and interbred with the ancestors of living humans (Meyer et al., 2012; Huerta-Sánchez et al., 2014). An analysis based on DNA methylation maps also suggested that morphologically, Denisovans should differ from modern humans, but show a high number of similarities with Neanderthals (Gokhman et al., 2019). The morphology of the XJY specimens is markedly different from that of early modern humans and shows some similarities to Neanderthals, which previously led to the proposal that they could represent Denisovans (Demeter et al., 2022). Previous metric studies have revealed Neanderthal-like characteristics in the bony labyrinth of XJY 6 (Wu et al., 2014, Fig. 1), but here we provide more detailed insights into this crucial anatomical structure using a geometric morphometric approach. Therefore, this study aims to compare the 3D shape of the bony labyrinth of XJY 6 with that of Early Pleistocene *Homo*, Neanderthals, and *Homo sapiens* to assess whether XJY falls within the range of one of the comparative groups, and/or if it could represent a Neanderthal or possibly a Denisovan.

2. Materials and methods

To elucidate the taxonomic relationships between the *Homo* fossils, XJY, and other human groups, we relied on a comparative sample comprising African Early Pleistocene *Homo*, *Homo erectus* s.s. (i.e., Asian *Homo erectus*, e.g., Antón et al., 2007) and Neanderthals, as well as Late Pleistocene and recent *H. sapiens* (Table 1). Information on the scans of XJY 6 and comparative samples can be found in Supplementary Online Material (SOM) Table S1. The bony labyrinth of all the individuals was segmented in Avizo v. 7.1 (FEI Visualization Sciences Group, Hillsboro) and Mimics v. 23.0 (Materialise, Leuven) using a semi-automatic approach based on grey value thresholding, with manual corrections when sediments were filling the canal lumen. Shape analyses were carried out in R v. 4.3.1 (R Core Team, 2023) using the packages 'geomorph' v. 4.0.6 (Baken et al., 2021), 'Morpho' v. 2.11 (Schlager, 2017), and 'ggplot2' v. 3.4.4 (Wickham, 2016).

For the full bony labyrinth analysis, a total of 148 landmarks and semilandmarks (SOM Fig. S1; SOM Table S2) were placed along the outer surface of the common crus, semicircular canals, and cochlea. The landmark configuration is inspired by those of Beaudet et al. (2019) and Gunz et al. (2012), differing only in the slightly smaller number of

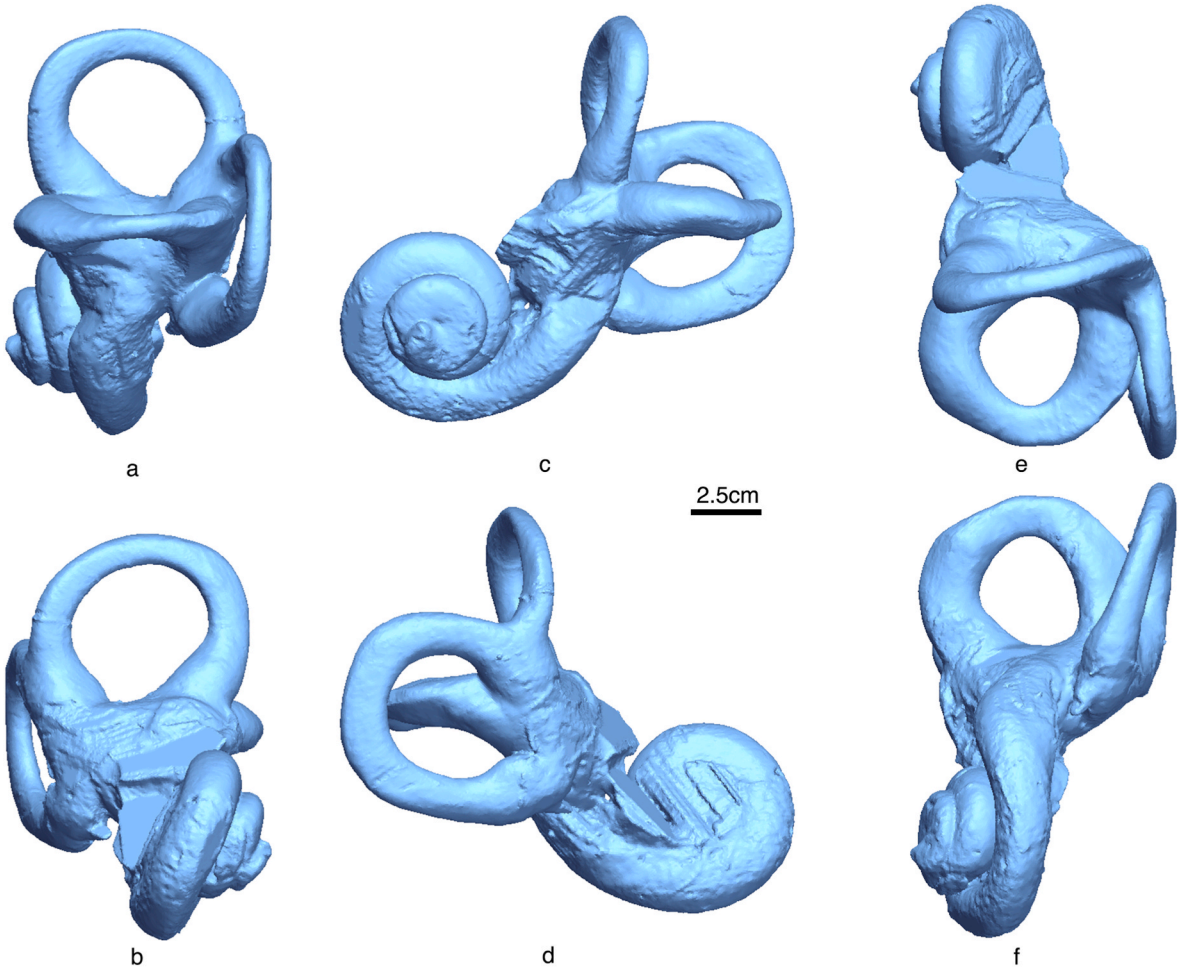

Fig. 1. The bony labyrinth of XJY 6 in posterior (a), anterior (b), lateral (c), medial (d), superior (e), and inferior views (f).

Table 1
Analytical sample composition and chronological context.

Group	Sample composition	Chronology
Xujiayao	Xujiayao 6	200–160 ka (Li et al., 2014)
African Early Pleistocene *Homo* ($n = 2$)	SK 27, SK 847	2.2–1.8 Ma (Pickering et al., 2011)
Homo erectus s.s. ($n = 4$)	Sangiran 2, 4	1.4 Ma or 0.9 Ma (Matsu'ura et al., 2020)
	Hexian	0.41 Ma (Grün et al., 1998)
	Lantian	1.63 Ma (Zhu et al., 2015)
Neanderthals ($n = 14$)	Engis 2	44.2–40.6 ka (Devièse et al., 2021)
	Gibraltar 1	42 ka (Wood et al., 2013)
	Krapina 38.1, 38.12, 38.20, 38.21, 39.1, 39.13, 39.18, 39.20, 39.3	130–120 ka (Rink et al., 1995)
	La Ferrassie 1, La Ferrassie 2	54-40 ka (Guérin et al., 2015)
	Tabun C1	143–112 ka (Grün and Stringer, 2000)
Homo sapiens ($n = 20$)	Longlin	14.3–11.5 ka (Curnoe et al., 2012)
	Ziyang	39–37 ka (Li and Zhang, 1984)
	Asian, African, and European extant humans	Modern (Dayal et al., 2009; Zhang and Schepartz, 2021)

semilandmarks for the canals and cochlea, which nonetheless allows to adequately capture patterns of shape variation (e.g., Perier et al., 2016). In addition, we conducted an analysis restricted to the semicircular canals (total of 98 landmarks and semilandmarks) to better understand the similarities between XJY 6 and the analyzed groups. Generalized Procrustes alignments were performed on the landmarks and equidistant semilandmarks (as in Beaudet et al., 2019; but see Gunz et al., 2012) to allow shape analysis with the function 'gpagen'. Landmarks and semilandmarks were placed by the same author (Y.Z.) to avoid inter-observer error. Intra-observer error was assessed by repeating landmark placement three times at different times for randomly selected individuals. This subset was Procrustes aligned and inspected by means of principal component analysis to ensure that differences between landmarking iterations are negligible (SOM Fig. S2).

We computed standard and cross-validated between group principal component analyses (bgPCA and CV-bgPCA) with the 'groupPCA' function, using Early Pleistocene *Homo* (African Early Pleistocene *Homo* sp. + *H. erectus* s.s.), Neanderthals, and *H. sapiens* as grouping factors, on the Procrustes aligned landmark data to inspect the patterns of shape variation occurring in the sample. The CV-bgPCA was used to ensure the absence of spurious grouping (Cardini and Polly, 2020) in the obtained results (SOM Figs. S3 and S4). The landmark configuration of XJY 6 was projected a posteriori into the shape space both in the full labyrinth and semicircular canal only analyses. We computed the typicality probability of XJY for each group with the 'typprobClass' function, the latter describing whether XJY 6 could be considered as an outlier for each of the groups (note that these probabilities are given as *p*-values for the null hypothesis of group membership and do not sum up to 100%). The shape changes along major bgPCA axes were visualized via superimposed landmark wireframes.

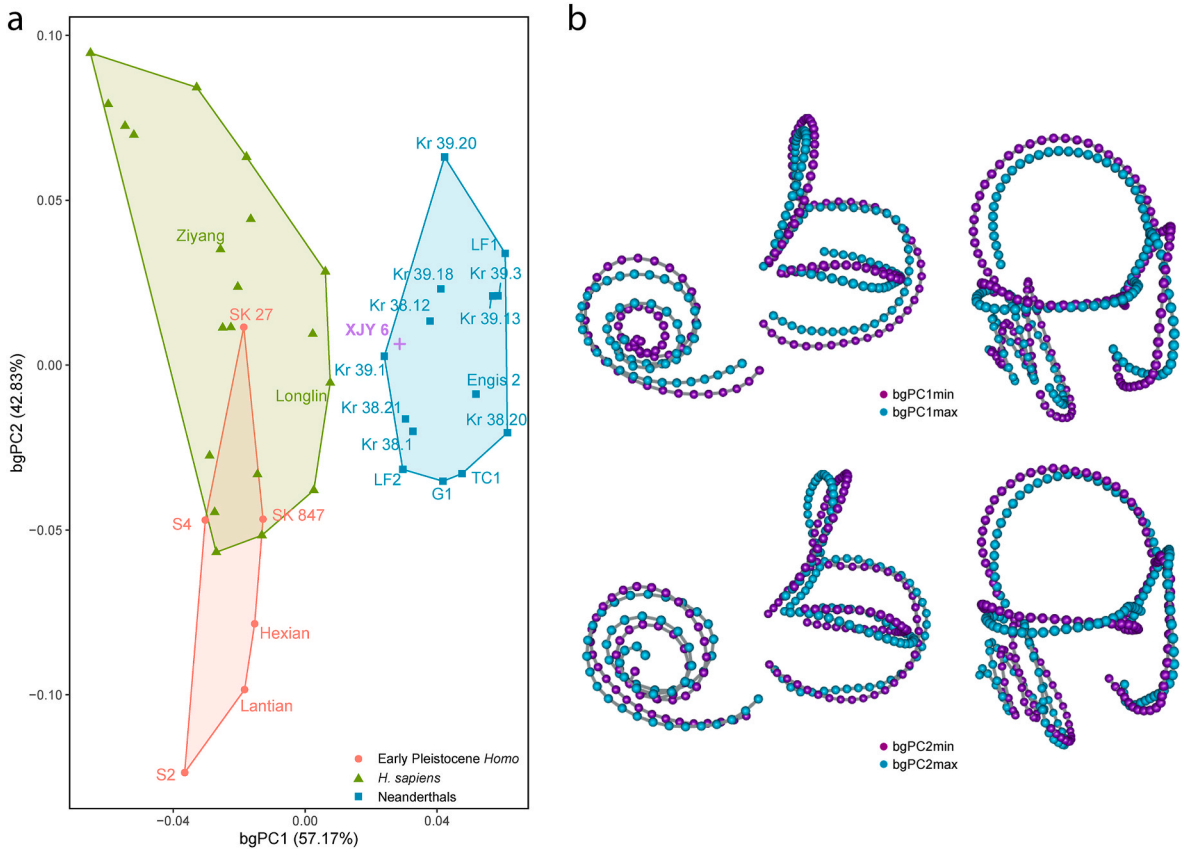

Fig. 2. Scatterplot of the first two between group principal components (bgPCs; a). Wireframes of the full landmark configuration show shape changes along bgPC1 and bgPC2 (b). Purple and cyan configurations correspond to maximum and minimum of each bgPC. Specimen abbreviations: Kr = Krapina, S = Sangiran, TC = Tabun, G = Gibraltar, LF = La Ferrassie. (For interpretation of the references to colour in this figure legend, the reader is referred to the Web version of this article).

3. Results

The results of the bgPCA reveal the distinctiveness of Neanderthals from *H. sapiens* and Early Pleistocene *Homo* (Fig. 2). *Homo sapiens* and both African Early Pleistocene *Homo* and *H. erectus* s.s. have similar negative bgPC1 scores due to the possession of large anterior and posterior canals, a small and low positioned lateral canal, a vertically oriented and medially positioned cochlear coiling, as well as a wide first cochlear turn and tightly coiled second and third turns. Neanderthals are well separated from the other groups along bgPC1, with a more superiorly positioned lateral canal (as the result of the rotation of both lateral canal and posterior canals forming an acute angle among them), a vertically inclined anterior ampulla, a very short and stout common crus, somewhat small anterior and posterior canals, and a tight first cochlear turn. Early Pleistocene *Homo* (especially *H. erectus* s.s.) is separated from Neanderthals and *H. sapiens* along bgPC2 due to their more anteriorly positioned anterior semicircular canal, and shorter cochlea with fewer turns. In both bgPC1 and bgPC2, XJY 6 clusters with Neanderthals, showing similar morphological. This result is further confirmed by the typicality probabilities obtained for XJY 6, showing that it is compatible with the group distribution of Neanderthals (SOM Table S3).

The analysis of the semicircular canals (Fig. 3) is consistent with the results obtained for the full configuration (Fig. 2). The pattern captured

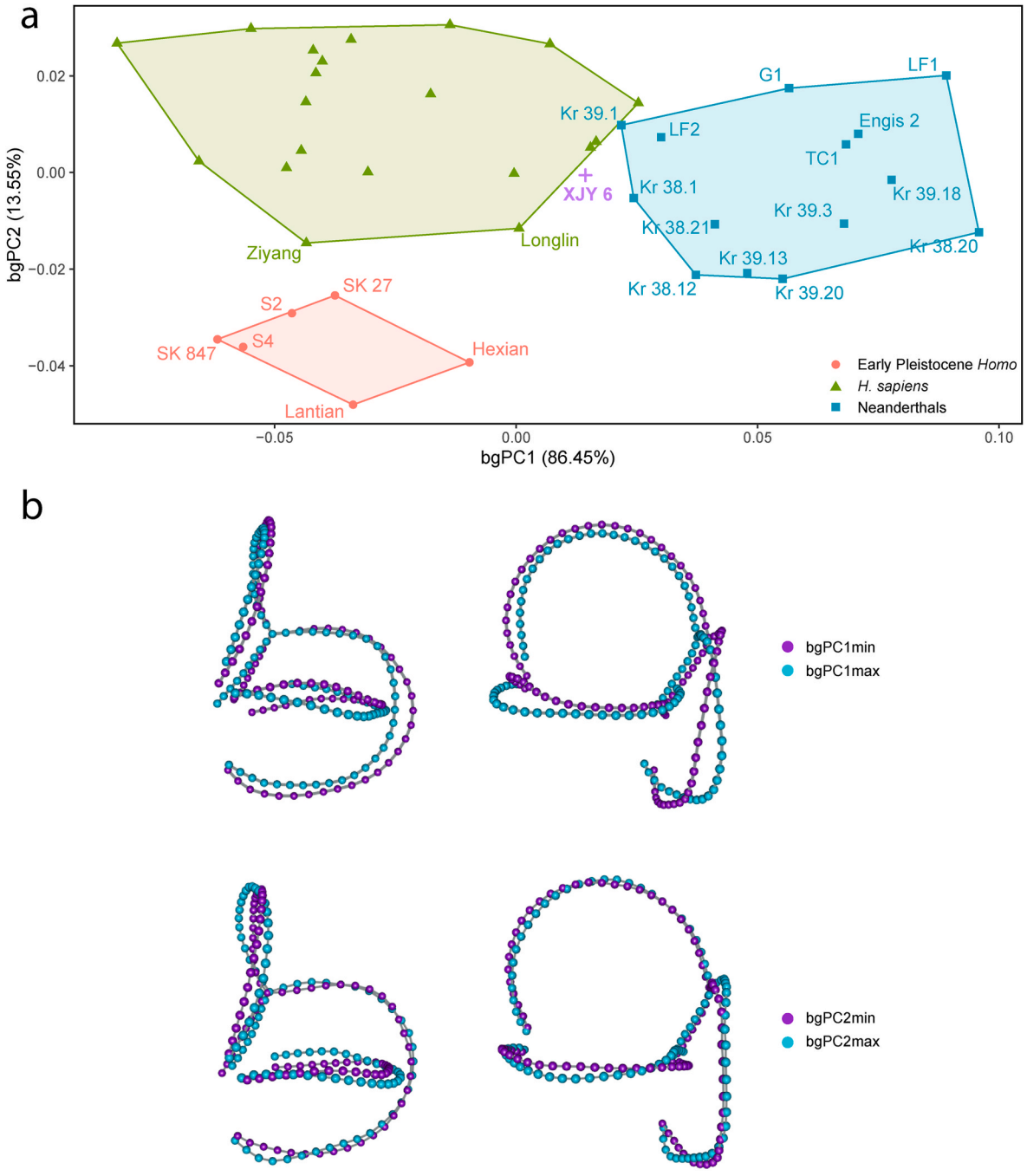

Fig. 3. Scatterplot of the first two between-group principal components (bgPCs; a) with the extreme shapes of the semicircular canal landmark configurations between bgPC1 minimum (purple) and bgPC1 maximum (cyan), as well as bgPC2 minimum (purple) and bgPC2 maximum (cyan; b). Specimen abbreviations: Kr = Krapina, S = Sangiran, TC = Tabun, G = Gibraltar, LF = La Ferrassie. (For interpretation of the references to colour in this figure legend, the reader is referred to the Web version of this article).

by the first two bgPCs mirrors that obtained with the full bony labyrinth, although the differences between *H. sapiens* and Neanderthals are reduced, and Early Pleistocene *Homo* is separated from *H. sapiens* on bgPC2. Also, XJY 6 falls outside the convex hull of Neanderthals and lies between them and *H. sapiens*. This is caused by two facts. First, compared to the whole configuration, modern humans show wider shape variation in the semicircular canals, which hampers identifying nuanced differences with Neanderthals in the first bgPC. Second, the shape of the cochlea and its position relative to the canals in XJY 6 are good indicators of its Neanderthal affinities. Nonetheless, typicality probabilities attribute XJY 6 to Neanderthals, although similarities with *Homo sapiens* are recovered (SOM Table S3).

4. Discussion and conclusions

The distinct labyrinth morphology that differentiates Neanderthals from Early Pleistocene *Homo* and *H. sapiens* observed in this study aligns with previous morphometric analyses, showing that Neanderthals have a more elevated position of the lateral semicircular canal, a larger lateral semicircular canal, a narrower anterior canal, a shorter posterior canal, and a more vertically inclined ampulla line (Hublin et al., 1996; Spoor et al., 2003; Wu et al., 2014). However, geometric morphometrics allowed us to confirm that additional features distinguish these groups. In particular, the elevated position of the lateral semicircular canal is a composite character influenced by both the orientation of the lateral and posterior canals. These two canals also exhibit more torsion in Early Pleistocene *Homo* and *H. sapiens* compared to Neanderthals. The present analyses show that the angle between the lateral and posterior planes of the semicircular canals and the orientation of the basal turn of the cochlea also differ between Neanderthals and other groups. Given the strong phylogenetic signal embedded in bony labyrinth shape (Spoor and Zonneveld, 1998; Lebrun et al., 2010; Urciuoli et al., 2020, 2021) and its importance for assessing dispersal distances in humans (Ponce de León et al., 2018), the present results based on inner ear morphology suggest a close phylogenetic relationship between XJY 6 and Neanderthals, and, by extension, possibly between XJY 6 and Denisovans. Consistent with a number of observed dental and cranial features, bony labyrinth morphology provides indications to connect the XJY specimens to Denisovans. As shown by paleogenetic analyses, Neanderthals and Denisovans are sister-groups (Meyer et al., 2012; Slon et al., 2018), and they likely share a number of morphological features (Demeter et al., 2022), but also probably differ in some cranial traits (Gokhman et al., 2019). The XJY cranial remains show a mosaic of Neanderthal-like traits and more primitive morphology as found in some Early and Middle Pleistocene *Homo* (Wu et al., 2012, 2013, 2014), together with a large cranial capacity exceeding the average value of Neanderthals (Wu et al., 2022). The shape of a Denisovan parietal bone from Denisova Cave has been suggested to be similar to that of the XJY fossils (Viola et al., 2019). The mandibular morphology of XJY 14 displays Neanderthal-like features (an asymmetrical mandibular notch, an enlarged superior medial pterygoid tubercle), as well as an unusual depression in the planum triangulare (Wu and Trinkaus, 2014). Dental morphology also aligns the XJY fossils with those from Denisova Cave. The M^2 PA1480 from XJY (Xing et al., 2015) is nearly identical in size and occlusal morphology to Denisova 4 (Sawyer et al., 2015). The enamel-dentine junction of the lower molar PA1500 (Xing et al., 2015) also strongly resembles that of the M_2 of the Xiahe mandible (Chen et al., 2019) and the isolated molar TNH2-1 (Demeter et al., 2022), both regarded as Denisovan specimens. Collectively, the discrepancies in cranial shape between XJY humans and Neanderthals, the morphological similarities of the XJY fossils with the few clearly identified Denisovan remains, and the absence of Neanderthals in Eastern Asia, suggest that these individuals very likely represent Denisovans.

The attribution of XJY humans to Denisovans has consequences for our understanding of human bony labyrinth evolution. Since most Neanderthal features in the bony labyrinth are not found in early Neanderthals, as highlighted by the Sima de los Huesos hominins (Quam et al., 2016; Conde-Valverde et al., 2023; Velez et al., 2023) and other Middle Pleistocene specimens (Spoor et al., 2003; Wu et al., 2014; Quam et al., 2016; Conde-Valverde et al., 2018), their presence in Denisovans would imply that it does not represent a retention of the plesiomorphic condition of the clade and must have been acquired after their split from Neanderthals (i.e., <500 ka; Meyer et al., 2016). One hypothesis is that the Neanderthal-like lateral canal morphology might have been present in the last common ancestor, but lost by the Sima de los Huesos hominins, possibly as a consequence of genetic drift related to a bottleneck that happened around 500–400 ka (Rogers et al., 2017). The evidence provided by another Iberian individual from the Gruta de Aroeira and dated to ca. 400 ka (Conde-Valverde et al., 2018) suggests that it belonged to a population with no clear similarities with Sima de los Huesos hominins, but that it was also lacking the typical Neanderthal-like canal morphology. The condition of these earliest known members of the Neanderthal lineage questions about the chronogeographic timing of fixation of this trait in the Neanderthal–Denisovan clade. Assuming that the XJY hominins are Denisovans, the markedly Neanderthal-like morphology of the inner ear could have been inherited from the last common ancestor of these groups. It is also possible that this trait evolved independently in both Neanderthals and Denisovans, or that it resulted from interbreeding between these Asian *Homo* groups and Neanderthals that occurred later than 200 ka, i.e., after the onset of a full set of Neanderthal characters in the bony labyrinth (Hill et al., 2014). While we cannot discount the former hypotheses based on the available data, the latter is largely in accordance with the results from molecular analyses of Asian Late Pleistocene Neanderthals and Denisovans suggesting frequent admixture among them (Prüfer et al., 2014; Slon et al., 2018). Given the remarkable morphological variability of eastern Asian Middle Pleistocene humans (Ni et al., 2021; Roksandic et al., 2022; Bae et al., 2023a, 2023b), further studies based on additional craniodental features and molecular analyses will be necessary to confirm the attribution of the XJY fossils to Denisovans and their phylogenetic relationships with Middle to Late Pleistocene *Homo*.

Data availability statement

The data that support the findings of this study are available from the corresponding author upon reasonable request.

CRediT authorship contribution statement

Yameng Zhang: Writing – review & editing, Writing – original draft, Visualization, Software, Methodology, Investigation, Funding acquisition, Formal analysis, Data curation, Conceptualization. **Alessandro Urciuoli:** Writing – review & editing, Software, Resources, Funding acquisition, Formal analysis, Data curation, Conceptualization. **Clément Zanolli:** Writing – review & editing, Validation, Software, Conceptualization. **Ottmar Kullmer:** Writing – review & editing, Data curation. **Xiujie Wu:** Writing – review & editing, Software, Funding acquisition, Data curation.

Declaration of competing interest

The authors declare that they have no known competing financial interests or personal relationships that could have appeared to influence the work reported in this paper.

Acknowledgments

We thank the Evolutionary Studies Institute (University of Witwatersrand, Johannesburg, South Africa), South African Nuclear Energy Corporation (NECSA, Pretoria, South Africa), Max Planck Institute for Evolutionary Anthropology (Leipzig, Germany), the Natural History

Museum of London (London, UK), the Museum National d'Histoire Naturelle (Paris, France) for scanning facilities; Nespos database for providing scanning data. We express our gratitude to the Werner Reimers Foundation in Bad Homburg, which provides the Gustav Heinrich Ralph von Koenigswald collection on permanent loan for scientific research to the Senckenberg Research Institute and Natural History Museum, Frankfurt. We are grateful to the Editor-in-Chief (Andrea Taylor), the Associate Editor, and the three reviewers (Philipp Gunz and two anonymous ones) for providing comments that helped us improve a previous draft of this paper. The research was supported by the National Natural Science Foundation of China (42102005, 42372001), by the Generalitat de Catalunya/CERCA Programme, and a Margarita Salas postdoctoral fellowship funded by the European Union NextGenerationEU to A.U. The funders had no role in the analysis, the interpretation of the results, the preparation of the manuscript nor the decision to publish.

Appendix A. Supplementary data

Supplementary Online Material to this article can be found online at https://doi.org/10.1016/j.jhevol.2024.103514.

References

Antón, S.C., Spoor, F., Fellmann, C.D., Swisher III, C.C., 2007. Defining *Homo erectus*: Size considered. In: Henke, W., Tattersall, I. (Eds.), Handbook of Paleoanthropology. Springer, Berlin, pp. 1655–1693.

Ao, H., Liu, C.-R., Roberts, A.P., Zhang, P., Xu, X., 2017. An updated age for the Xujiayao hominin from the Nihewan Basin, North China: Implications for Middle Pleistocene human evolution in East Asia. J. Hum. Evol. 106, 54–65.

Arsuaga, J.L., Martínez, I., Arnold, L.J., Aranburu, A., Gracia-Téllez, A., Sharp, W.D., Quam, R.M., Falguères, C., Pantoja-Pérez, A., Bischoff, J., Poza-Rey, E., Parés, J.M., Carretero, J.M., Demuro, M., Lorenzo, C., Sala, N., Martinón-Torres, M., García, N., Velasco, A.A.d., Cuenca-Bescós, G., Gómez-Olivencia, A., Moreno, D., Pablos, A., Shen, C.C., Rodríguez, L., Ortega, A.I., García, R., Bonmatí, A., Bermúdez de Castro, J.M., Carbonell, E., 2014. Neandertal roots: Cranial and chronological evidence from Sima de los Huesos. Science 344, 1358–1363.

Bae, C.J., Aiello, L.C., Hawks, J., Kaifu, Y., Lindal, J., Martinón-Torres, M., Ni, X., Posth, C., Radović, P., Reed, D., Schroeder, L., Schwartz, J.H., Silcox, M.T., Welker, F., Wu, X.-J., Zanolli, C., Roksandic, M., 2023a. Moving away from "the Muddle in the Middle" toward solving the Chibanian puzzle. Evol. Anthropol. 33, e22011.

Bae, C.J., Liu, W., Wu, X., Zhang, Y., Ni, X., 2023b. "Dragon man" prompts rethinking of Middle Pleistocene hominin systematics in Asia. Innovation 4, 100527.

Baken, E., Collyer, M., Kaliontzopoulou, A., Adams, D., 2021. geomorph v4.0 and gmShiny: Enhanced analytics and a new graphical interface for a comprehensive morphometric experience. Methods Ecol. Evol. 12, 2355–2363.

Beaudet, A., Clarke, R.J., Bruxelles, L., Carlson, K.J., Crompton, R., de Beer, F., Dhaene, J., Heaton, J.L., Jakata, K., Jashashvili, T., Kuman, K., McClymont, J., Pickering, T.R., Stratford, D., 2019. The bony labyrinth of StW 573 ("Little Foot"): Implications for early hominin evolution and paleobiology. J. Hum. Evol. 127, 67–80.

Cardini, A., Polly, P.D., 2020. Cross-validated between group PCA scatterplots: A solution to spurious grouping separation? Evol. Biol. 47, 85–95.

Chen, T., Yuan, S., Gao, S., 1984. The study on uranium-series dating of fossil bones as an absolute age sequence for the main Paleolithic sites of North China. Acta Anthropol. Sin. 3, 259–269.

Chen, F., Welker, F., Shen, C.-C., Bailey, S.E., Bergmann, I., Davis, S., Xia, H., Wang, H., Fischer, R., Freidline, S.E., Yu, T.-L., Skinner, M.M., Stelzer, S., Dong, G., Fu, Q., Dong, G., Wang, J., Zhang, D., Hublin, J.J., 2019. A late Middle Pleistocene Denisovan mandible from the Tibetan Plateau. Nature 569, 409–412.

Conde-Valverde, M., Quam, R., Martinez, I., Arsuaga, J.L., Daura, J., Sanz, M., Zilhao, J., 2018. The bony labyrinth in the Aroeira 3 Middle Pleistocene cranium. J. Hum. Evol. 124, 105–116.

Conde-Valverde, M., Martínez, I., Quam, R., Arsuaga, J.L., 2023. The ear of the Sima de los Huesos hominins (Atapuerca, Spain). Anat. Rec. 2023, 1–15.

Curnoe, D., Xueping, J., Herries, A.I., Kanning, B., Taçon, P.S., Zhende, B., Fink, D., Yunsheng, Z., Hellstrom, J., Yun, L., 2012. Human remains from the Pleistocene-Holocene transition of southwest China suggest a complex evolutionary history for East Asians. PLoS One 7, e31918.

Dayal, M.R., Kegley, A.D., Štrkalj, G., Bidmos, M.A., Kuykendall, K.L., 2009. The history and composition of the Raymond A. Dart Collection of human skeletons at the University of the Witwatersrand, Johannesburg, South Africa. Am. J. Phys. Anthropol. 140, 324–335.

Demeter, F., Zanolli, C., Westaway, K.E., Joannes-Boyau, R., Duringer, P., Morley, M.W., Welker, F., Rüther, P.L., Skinner, M.M., McColl, H., Gaunitz, C., Vinner, L., Dunn, T. E., Olsen, J.V., Sikora, M., Ponche, J.-L., Suzzoni, E., Frangeul, S., Boesch, Q., Antoine, P.-O., Pan, L., Xing, S., Zhao, J.-X., Bailey, R.M., Boualaphane, S., Sichanthongtip, P., Sihanam, D., Patole-Edoumba, E., Aubaile, F., Crozier, F., Bourgon, N., Zachwieja, A., Luangkhoth, T., Souksavatdy, V., Sayavongkhamdy, T., Cappellini, E., Bacon, A.-M., Hublin, J.-J., Willerslev, E., Shackelford, L., 2022. A Middle Pleistocene Denisovan molar from the Annamite Chain of northern Laos. Nat. Commun. 13, 2557.

Devièse, T., Abrams, G., Hajdinjak, M., Pirson, S., De Groote, I., Di Modica, K., Toussaint, M., Fischer, V., Comeskey, D., Spindler, L., Meyer, M., Semal, P., Higham, T., 2021. Reevaluating the timing of Neanderthal disappearance in Northwest Europe. Proc. Natl. Acad. Sci. USA 118, e2022466118.

Franciscus, R.G., 2003. Internal nasal floor configuration in *Homo* with special reference to the evolution of Neandertal facial form. J. Hum. Evol. 44, 701–729.

Gokhman, D., Mishol, N., de Manuel, M., de Juan, D., Shuqrun, J., Meshorer, E., Marques-Bonet, T., Rak, Y., Carmel, L., 2019. Reconstructing Denisovan anatomy using DNA methylation maps. Cell 179, 180–192.

Gómez-Robles, A., 2019. Dental evolutionary rates and its implications for the Neanderthal–modern human divergence. Sci. Adv. 5, eaaw1268.

Grün, R., Huang, P.-H., Huang, W., McDermott, F., Thorne, A., Stringer, C.B., Yan, G., 1998. ESR and U-series analyses of teeth from the palaeoanthropological site of Hexian, Anhui Province, China. J. Hum. Evol. 34, 555–564.

Grün, R., Stringer, C., 2000. Tabun revisited: Revised ESR chronology and new ESR and U-series analyses of dental material from Tabun C1. J. Hum. Evol. 39, 601–612.

Guérin, G., Frouin, M., Talamo, S., Aldeias, V., Bruxelles, L., Chiotti, L., Dibble, H.L., Goldberg, P., Hublin, J.-J., Jain, M., Lahaye, C., Madelaine, S., Maureille, B., McPherron, S.J.P., Mercier, N., Murray, A.S., Sandgathe, D., Steele, T.E., Thomsen, K.J., Turq, A., 2015. A multi-method luminescence dating of the Palaeolithic sequence of La Ferrassie based on new excavations adjacent to the La Ferrassie 1 and 2 skeletons. J. Archaeol. Sci. 58, 147–166.

Gunz, P., Ramsier, M., Kuhrig, M., Hublin, J.J., Spoor, F., 2012. The mammalian bony labyrinth reconsidered, introducing a comprehensive geometric morphometric approach. J. Anat. 220, 529–543.

Hill, C.A., Radovčić, J., Frayer, D.W., 2014. Brief communication: Investigation of the semicircular canal variation in the Krapina Neandertals. Am. J. Phys. Anthropol. 154, 302–306.

Hublin, J.-J., Spoor, F., Braun, M., Zonneveld, F., Condemi, S., 1996. A late Neanderthal associated with Upper Palaeolithic artefacts. Nature 381, 224–226.

Huerta-Sánchez, E., Jin, X., Asan, Bianba, Z., Peter, B.M., Vinckenbosch, N., Liang, Y., Yi, X., He, M., Somel, M., Ni, P., Wang, B., Ou, X., Huasang, Luosang, J., Cuo, Z.X.P., Li, K., Gao, G., Yin, Y., Wang, W., Zhang, X., Xu, X., Yang, H., Li, Y., Wang, J., Wang, J., Nielsen, R., 2014. Altitude adaptation in Tibetans caused by introgression of Denisovan-like DNA. Nature 512, 194–197.

Li, X., Zhang, S., 1984. Paleoliths discovered in Ziyang man locality B. Acta Anthropol. Sin. 3, 215–224 (in Chinese).

Lebrun, R., Ponce de León, M., Tafforeau, P., Zollikofer, C., 2010. Deep evolutionary roots of strepsirrhine primate labyrinthine morphology. J. Anat. 216, 368–380.

Li, Z., Xu, Q., Zhang, S., Hun, L., Li, M., Xie, F., Wang, F., Liu, L., 2014. Study on stratigraphic age, climate changes and environment background of Houjiayao Site in Nihewan Basin. Quat. Int. 349, 42–48.

Liu, W., Schepartz, L.A., Xing, S., Miller-Antonio, S., Wu, X., Trinkaus, E., Martinón-Torres, M., 2013. Late Middle Pleistocene hominin teeth from Panxian Dadong, South China. J. Hum. Evol. 64, 337–355.

Matsu'ura, S., Kondo, M., Danhara, T., Sakata, S., Iwano, H., Hirata, T., Kurniawan, I., Setiyabudi, E., Takeshita, Y., Hyodo, M., Kitaba, I., Sudo, M., Danhara, Y., Aziz, F., 2020. Age control of the first appearance datum for Javanese *Homo erectus* in the Sangiran area. Science 367, 210–214.

Meyer, M., Kircher, M., Gansauge, M.-T., Li, H., Racimo, F., Mallick, S., Schraiber, J.G., Jay, F., Prüfer, K., de Filippo, C., Sudmant, P.H., Alkan, C., Fu, Q., Do, R., Rohland, N., Tandon, A., Siebauer, M., Green, R.E., Bryc, K., Briggs, A.W., Stenzel, U., Dabney, J., Shendure, J., Kitzman, J., Hammer, M.F., Shunkov, M.V., Derevianko, A.P., Patterson, N., Andres, A.M., Eichler, E.E., Slatkin, M., Reich, D., Kelso, J., Pääbo, S., 2012. A high-coverage genome sequence from an archaic Denisovan. Science 338, 222–226.

Meyer, M., Fu, Q., Aximu-Petri, A., Glocke, I., Nickel, B., Arsuaga, J.-L., Martínez, I., Gracia, A., de Castro, J.M.B., Carbonell, E., Pääbo, S., 2014. A mitochondrial genome sequence of a hominin from Sima de los Huesos. Nature 505, 403–406.

Meyer, M., Arsuaga, J.-L., de Filippo, C., Nagel, S., Aximu-Petri, A., Nickel, B., Martínez, I., Gracia, A., de Castro, J.M.B., Carbonell, E., Viola, B., Kelso, J., Prüfer, K., Pääbo, S., 2016. Nuclear DNA sequences from the Middle Pleistocene Sima de los Huesos hominins. Nature 531, 504.

Ni, X., Ji, Q., Wu, W., Shao, Q., Ji, Y., Zhang, C., Liang, L., Ge, J., Guo, Z., Li, J., Li, Q., Grün, R., Stringer, C., 2021. Massive cranium from Harbin in northeastern China establishes a new Middle Pleistocene human lineage. Innovation 2, 100130.

Norton, C.J., Gao, X., 2008. Hominin–carnivore interactions during the Chinese Early Paleolithic: Taphonomic perspectives from Xujiayao. J. Hum. Evol. 55, 164–178.

Perier, A., Lebrun, R., Marivaux, L., 2016. Different level of intraspecific variation of the bony labyrinth morphology in slow- versus fast-moving primates. J. Mamm. Evol. 23, 353–368.

Pickering, R., Kramers, J.D., Hancox, P.J., de Ruiter, D.J., Woodhead, J.D., 2011. Contemporary flowstone development links early hominin bearing cave deposits in South Africa. Earth Planet. Sci. Lett. 306, 23–32.

Ponce de León, M.S., Koesbardiati, T., Weissmann, J.D., Milella, M., Reyna-Blanco, C.S., Suwa, G., Kondo, O., Malaspinas, A.-S., White, T.D., Zollikofer, C.P., 2018. Human bony labyrinth is an indicator of population history and dispersal from Africa. Proc. Natl. Acad. Sci. USA 115, 4128–4133.

Prüfer, K., Racimo, F., Patterson, N., Jay, F., Sankararaman, S., Sawyer, S., Heinze, A., Renaud, G., Sudmant, P.H., de Filippo, C., Li, H., Mallick, S., Dannemann, M., Fu, Q., Kircher, M., Kuhlwilm, M., Lachmann, M., Meyer, M., Ongyerth, M., Siebauer, M., Theunert, C., Tandon, A., Moorjani, P., Pickrell, J., Mullikin, J.C., Vohr, S.H.,

Green, R.E., Hellmann, I., Johnson, P.L.F., Blanche, H., Cann, H., Kitzman, J.O., Shendure, J., Eichler, E.E., Lein, E.S., Bakken, T.E., Golovanova, L.V., Doronichev, V. B., Shunkov, M.V., Derevianko, A.P., Viola, B., Slatkin, M., Reich, D., Kelso, J., Pääbo, S., 2014. The complete genome sequence of a Neanderthal from the Altai Mountains. Nature 505, 43–49.

Quam, R., Lorenzo, C., Martínez, I., Gracia-Téllez, A., Arsuaga, J.L., 2016. The bony labyrinth of the middle Pleistocene Sima de los Huesos hominins (Sierra de Atapuerca, Spain). J. Hum. Evol. 90, 1–15.

R Core Team, 2023. R: A language and environment for statistical computing. R Foundation for Statistical Computing, Vienna.

Rink, W.J., Schwarcz, H.P., Smith, F.H., Radovčić, J., 1995. ESR ages for Krapina hominids. Nature 378, 24–24.

Roksandic, M., Radovic, P., Wu, X.J., Bae, C.J., 2022. Resolving the "muddle in the middle": The case for *Homo bodoensis* sp. nov. Evol. Anthropol. 31, 20–29.

Rogers, A.R., Bohlender, R.J., Huff, C.D., 2017. Early history of Neanderthals and Denisovans. Proc. Natl. Acad. Sci. USA 114, 9859–9863.

Sawyer, S., Renaud, G., Viola, B., Hublin, J.J., Gansauge, M.T., Shunkov, M.V., Derevianko, A.P., Prüfer, K., Kelso, J., Pääbo, S., 2015. Nuclear and mitochondrial DNA sequences from two Denisovan individuals. Proc. Natl. Acad. Sci. USA 112, 15696–15700.

Schlager, S., 2017. Morpho and Rvcg – shape analysis in R: R-packages for geometric morphometrics, shape analysis and surface manipulations. In: Zheng, G., Li, S., Székely, G. (Eds.), Statistical Shape and Deformation Analysis. Methods, Implementation and Applications. Academic Press, London, pp. 217–256.

Slon, V., Mafessoni, F., Vernot, B., de Filippo, C., Grote, S., Viola, B., Viola, B., Hajdinjak, M., Peyrégne, S., Nagel, S., Brown, S., Douka, K., Douka, K., Higham, T., Kozlikin, M.B., Shunkov, M.V., Shunkov, M.V., Derevianko, A.P., Kelso, J., Meyer, M., Prüfer, K., Pääbo, S., 2018. The genome of the offspring of a Neanderthal mother and a Denisovan father. Nature 561, 113–117.

Spoor, F., Zonneveld, F., 1998. Comparative review of the human bony labyrinth. Yearb. Phys. Anthropol. 41, 211–251.

Spoor, F., Hublin, J.-J., Braun, M., Zonneveld, F., 2003. The bony labyrinth of Neanderthals. J. Hum. Evol. 44, 141–165.

Urciuoli, A., Zanolli, C., Beaudet, A., Dumoncel, J., Santos, F., Moyà-Solà, S., Alba, D.M., 2020. The evolution of the vestibular apparatus in apes and humans. eLife 3, e51261.

Urciuoli, A., Zanolli, C., Almécija, S., Beaudet, A., Dumoncel, J., Morimoto, N., Nakatsukasa, M., Moyà-Solà, S., Begun, D.R., Alba, D.M., 2021. Reassessment of the phylogenetic relationships of the late Miocene apes *Hispanopithecus* and *Rudapithecus* based on vestibular morphology. Proc. Natl. Acad. Sci. USA 118, e2015215118.

Velez, A.D., Quam, R., Conde-Valverde, M., Martínez, I., Lorenzo, C., Arsuaga, J.L., 2023. Geometric morphometric analysis of the bony labyrinth of the Sima de los Huesos hominins. J. Hum. Evol. 174, 103280.

Viola, B.T., Gunz, P., Neubauer, S., Slon, V., Kozlikin, M.B., Shunkov, M.V., Meyer, M., Pääbo, S., Derevianko, A.P., 2019. A parietal fragment from Denisova cave. Am. J. Phys. Anthropol. 168 (S68), 258.

Wickham, H., 2016. ggplot2: Elegant Graphics for Data Analysis. Springer-Verlag, New York.

Wood, R.E., Barroso-Ruíz, C., Caparrós, M., Jordá Pardo, J.F., Galván Santos, B., Higham, T.F.G., 2013. Radiocarbon dating casts doubt on the late chronology of the Middle to Upper Palaeolithic transition in southern Iberia. Proc. Natl. Acad. Sci. USA 110, 2781–2786.

Wu, X., Poirier, F.E., 1995. Human Evolution in China: A Metric Description of the Fossils and a Review of the Sites. Oxford University Press, New York.

Wu, X., Trinkaus, E., 2014. The Xujiayao 14 mandibular ramus and Pleistocene *Homo* mandibular variation. C. R. Palevol 13, 333–341.

Wu, X., Maddux, S.D., Pan, L., Trinkaus, E., 2012. Nasal floor variation among eastern Eurasian Pleistocene *Homo*. Anthropol. Sci. 120, 217–226.

Wu, X., Xing, S., Trinkaus, E., 2013. An enlarged parietal foramen in the late archaic Xujiayao 11 neurocranium from Northern China, and rare anomalies among Pleistocene *Homo*. PLoS One 8, e59587.

Wu, X., Crevecoeur, I., Liu, W., Xing, S., Trinkaus, E., 2014. Temporal labyrinths of eastern Eurasian Pleistocene humans. Proc. Natl. Acad. Sci. USA 111, 10509–10513.

Wu, X., Bae, C.J., Friess, M., Xing, S., Athreya, S., Liu, W., 2022. Evolution of cranial capacity revisited: A view from the late Middle Pleistocene cranium from Xujiayao, China. J. Hum. Evol. 163, 103119.

Xing, S., Martinón-Torres, M., Bermúdez de Castro, J.M., Wu, X., Liu, W., 2015. Hominin teeth from the early Late Pleistocene site of Xujiayao, Northern China: Xujiayao hominin teeth. Am. J. Phys. Anthropol. 156, 224–240.

Zhang, Y., Schepartz, L.A., 2021. Three-dimensional geometric morphometric studies of modern human occipital variation. PLoS One 16, e0245445.

Zhu, Z.-Y., Dennell, R., Huang, W.-W., Wu, Y., Rao, Z.-G., Qiu, S.-F., Xie, J.-B., Liu, W., Fu, S.-Q., Han, J.-W., Zhou, H.-Y., Ou Yang, T.-P., Li, H.-M., 2015. New dating of the *Homo erectus* cranium from Lantian (Gongwangling), China. J. Hum. Evol. 78, 144–157.